Measurements of Temperature Fields Within Film-Cooling Jets Injected from a Row of Compound Angle Holes

Sang Woo Lee*, Jong Ryul Byun and Dae Sung Lee*****

(Received December 21, 1996)

Thermal fields downstream of the film-cooling jets injected through compound angle holes in a row have been measured with variations of the orientation angle and the blowing ratio. Detailed temperature distributions within the heated jets are reported for four orientation angles of 0 deg, 30 deg, 60 deg and 90 deg with three blowing ratios of 0.5, 1.0 and 1.5. The inclination angle, span-to-diameter ratio and length-to-diameter of the injection holes are fixed at 30 deg, 3.0 and 4.0, respectively, throughout the experiments. The result shows that the increase of the orientation angle results in uniform spanwise film coverage and improved film-cooling performance. The compound angle effects are found to be dominant in the case that the orientation angle is larger than 60 deg, especially when the blowing ratio is higher than unity.

Key Words: Film Cooling, Compound Angle Hole, Temperature Field, Blowing Ratio

Nomenclature

D : Diameter of an injection hole
DR : Density ratio $=\rho_j/\rho_\infty$
h : Heat transfer coefficient, Eq. (1)
I : Momentum flux ratio $=\rho_j U_j^2/\rho_\infty U_\infty^2$
L : Length of an injection hole
M : Blowing ratio or mass flux ratio $=\rho_j U_j/\rho_\infty U_\infty$
q : Heat flux, Eq. (1)
Re_D : Reynolds number based on U_j and $D=U_jD/\nu_j$
$Re_{\delta 2}$: Reynolds number based on U_∞ and $\delta_2=U_\infty\delta_2/\nu_\infty$
S : Spanwise distance between adjacent injection holes
T : Temperature
T_{aw} : Adiabatic wall temperature
T_j : Temperature of jet measured inside the plenum in Fig. 1
T_{nw} : Near-wall temperature measured at $y/D=0.1$
T_w : Wall temperature
T_∞ : Freestream temperature of the mainflow
U_j : Spatially-averaged mean velocity across the injection hole
U_j : Freestream velocity of the mainflow
x : Coordinate in the streamwise direction, Fig. 1
y : Coordinate in the normal direction, Fig. 1
z : Coordinate in the spanwise direction, Fig. 1

Greek characters

α : Inclination angle of an injection hole, defined as the angle between the injection vector and its projection on x-z plane, Fig. 1
β : Orientation angle, defined as the angle between the x-axis and projection of the injection vector on x-z plane, Fig. 1
δ_2 : Momentum boundary-layer thickness
η : Film-cooling effectiveness, Eq. (2)
θ : Dimensionless temperature $=(T-T_\infty)/(T_j-T_\infty)$
θ_w : Dimensionless wall temperature $=(T_w-T_\infty)/(T_j-T_\infty)$

* Dept. of Mechanical Engrg., Kum-Oh National University of Technology
** Graduate school, Kum-Oh National University of Technology
*** Aeropropulsion Department, Korea Aerospace Research Institute

θ_{nw} : Dimensionless near-wall temperature $=(T_{nw}-T_\infty)/(T_j-T_\infty)$

ν_j : Kinematic viscosity of injectant inside the plenum in Fig. 1

ν_∞ : Kinematic viscosity of the mainflow

ρ_j : Density of injectant at the plenum in Fig. 1

ρ_∞ : Density of the mainflow

1. Introduction

A better cooling scheme to achieve the higher turbine inlet temperature has been one of the important subjects in the development of high-efficiency gas turbines. Film cooling is an effective cooling method to protect the gas turbine hot sections such as a combustor liner, turbine vanes and blades, introducing lower temperature air into the hot mainflow. Among many studies to improve the film-cooling performance, film cooling with compound angle orientations has been recently recognized as one of the most effective cooling methods. The compound angle film cooling is characterized by two injection angles, the inclination angle, α, and the orientation angle, β, as defined in the nomenclature and in Fig. 1.

Ligrani et al. (1992, 1994a and 1994b) studied the compound angle film coolings with various injection-hole geometries. They reported the detailed film-cooling effectivenesses and the heat transfer coefficients of film-cooled surfaces. Honami et al. (1994) studied the behavior of the laterally-injected jets with holes spaced at five hole diameter. They found that the laterally-injected jets showed an asymmetric structure with a large-scale vortex motion. Srinath et al. (1995a and 1995b) reported the heat transfer coefficients and the film effectiveness distributions over the flat surface with a row of compound angle holes. Three orientation angles of 0 deg, 45 deg and 90 deg with air ($DR=0.98$) and CO_2 ($DR=1.46$) as coolants were tested at an elevated freestream turbulence condition, using the transient liquid crystal technique. They found that the heat transfer coefficients increase for both coolants as the orientation angle increases from 0 deg to 90 deg, and that the compound angle injections provide higher film effectiveness than the simple angle injection ($\beta=0$ deg). Lee et al. (1997) investigated the flow characteristics and the aerodynamic loss distributions of the film-cooling jets with compound angle orientations. They showed that the increase of the orientation angle provided better film coverage on the test surface, but caused large flow disturbances in the mainflow.

Most of the open literatures on the film cooling through compound angle holes were focused mainly on the measurements of the film cooling effectiveness and the heat transfer coefficient. In addition to these primary data, systematic studies on the temperature distribution are still needed for better understanding of the thermal structure of the compound angle jet in a row. In this study, thermal field downstream of the compound angle holes has been investigated as a function of the orientation angle and the blowing ratio.

2. Experimental Apparatus and Procedure

The wind tunnel used in the present study was an open-circuit type with a cross-section of 0.6m $\times$0.4m. At a mean velocity of 15 m/s, uniformity and turbulent level were 1.0% and 0.5%, respectively. The uniform flow coming out of the wind-tunnel contraction body was developing to the turbulent boundary-layer flow on the floor of the test section after a trip wire of 1.8 mm in diameter, which was located 60 mm downstream of the wind-tunnel exit. Injection plates of thickness 40 mm were made of bakelite with the thermal conductivity of 1.4 W/(mK). With four different injection plates, the orientation angle, β, has been varied to be 0 deg, 30 deg, 60 deg and 90 deg. On each injection plate, seven compound angle holes of diameter 20 mm were drilled in a row as shown in Fig. 1.The centers of the holes were located 740 mm downstream of the trip wire. For all injection plates, the inclination angle, α, was fixed at 30 deg. Each exit of the injection hole had an elliptical shape. The major axis of the ellipse was 40 mm long and its minor axis was 20 mm long. The x, y and z were streamwise, normal and spanwise coordinates, respectively, with respect to the

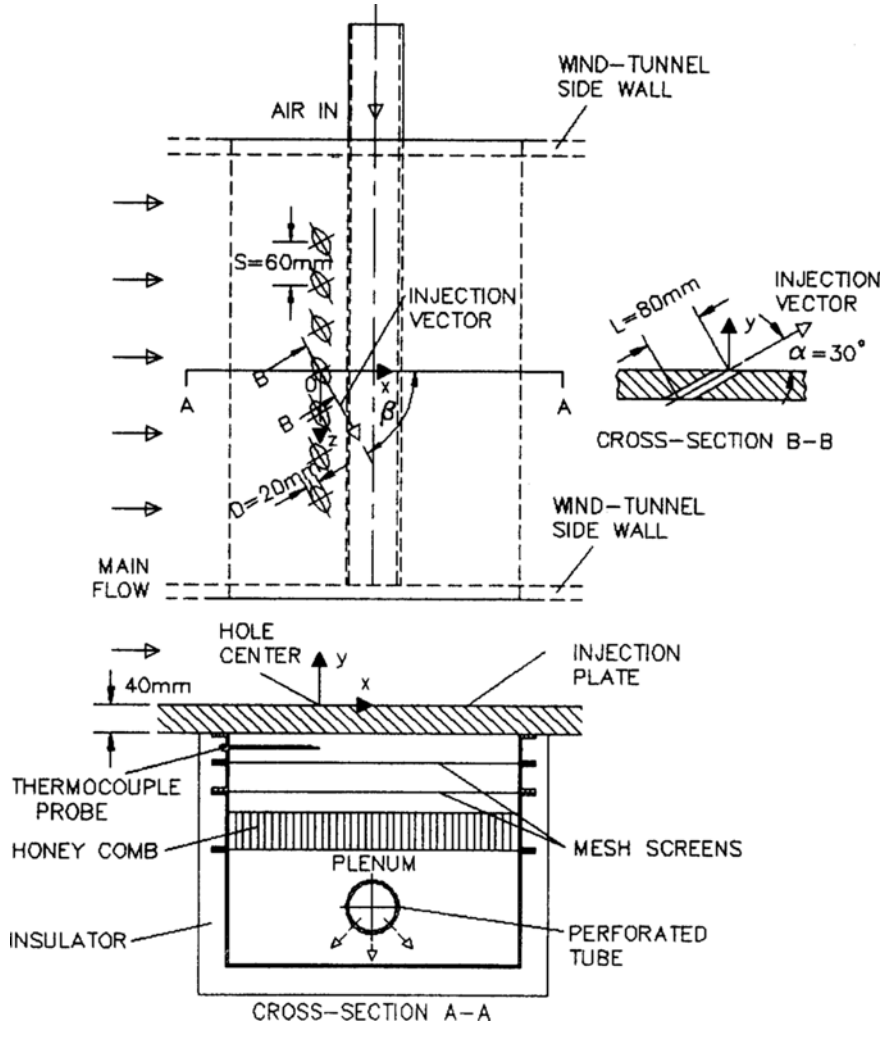

Fig. 1 Schematic diagram of injection plate with compound-angle holes in a row.

mainflow direction. The origin of the coordinates coincided with the center of the middle injection hole as shown in Fig. 1.

The injection air from a centrifugal blower was supplied to a perforated tube inside the plenum in Fig. 1 via a by-pass valve, an orifice, a flow control valve, an air heater with a proportional temperature controller and a mixing chamber in sequence. The mixing chamber of about 0.4 m^3 in volume was employed to smooth out possible temperature fluctuation. Before being injected into the cold mainflow, the heated air was uniformly distributed over seven film-cooling holes through the perforated tube, a honeycomb and two mesh screens. Present study employed a corner-tapping orifice based on ISO 5167(1991) to measure the injection-air flow rate.

In this experiment, a exposed-junction type thermocouple probe was used for the mean temperature measurements, which was fabricated with a T-type thermocouple wire (OMEGA, TT-T-30), and its beed size was about 0.7 mm in diameter. All the temperature measurements were based on the STP 470A(1974) published by ASTM. The probe was moved by an automatic probe traverse system, which was equipped with linear motion guides, stepping motors and stepping motor drivers. At each measurement loca-

tion, the voltage from the thermocouple probe as well as those from the thermocouples installed inside the plenum and in the mainflow were measured with a digital voltmeter (Keithley, Model 2001), which was controlled by a personal computer (IBM, AT 486) through a GPIB. The thermocouples were calibrated with a constant -temperature chamber (Fisher Scientific, Model 9010). Temperature data were finally obtained from the temperature-voltage calibration curves.

3. Experimental Conditions and Uncertainty

Freestream velocity of the mainflow, U_∞, measured at $x/D=0$ was maintained at 15 m/s. At the central hole site, boundary-layer thickness without injection was measured to be 19.3mm, and the displacement and momentum thicknesses were about 2.06 mm and 1.65 mm, respectively. Two-dimensionality of the mainflow boundary layer was assured by measuring the veocity profiles at four spanwise positions. The Reynolds number based on the freestream velocity and the momentum boundary-layer thickness, $Re_{\delta 2}$, was 1.6×10^3. When the blowing ratio was 1.0, the Reynolds number based on the spatially-averaged injection velocity and the hole diameter, Re_D, was 1.9×10^4. The temperature measurements were carried out in the cases that the orientation angles were 0 deg, 30 deg, 60 deg and 90 deg for the inclination angle of 30 deg. The temperature difference between the mainflow and jet was maintained at 25 degC. Thus, the density ratio of the two fluids was $DR=0.92$. The blowing ratio was changed to be $M=0.5$, 1.0 and 1.5, which were equivalent to $I=0.27$, 1.08 and 2.44, respectively. Throughout the experiments, the span-to -diameter ratio and length-to-diameter ratio of the film-cooling holes were kept to be $S/D=3.0$ and $L/D=4.0$, respectively. Temperatures were measured at 25 points in the z-direction with an interval of $D/4$ from $z/D=-3.0$ to $z/D=3.0$. In the y-direction, measurements were performed initially at $y=D/10$ and then, at additional 12 points with an interval of $D/4$, starting from $y=D/4$.

The uncertainty intervals presented in this study were evaluated with 95 percent confidence level (Kline and McClintock, 1953). Uncertainties associated with the probe location were ±0.1 mm in the x-direction and ±0.05 mm in the y- and z-directions. The uncertainty interval in the injection mass flow measurement was $\pm0.5\%$ of mass flow rate based on the uncertainty analysis of the ISO 5167(1991). The orifice measurement also showed a good agreement within 1%, compared with the result from a total-head probe. Uncertainties of the freestream temperature, T∞, the temperature of the injected jet, T_j, and the dimensionless temperature, θ, were estimated to be ±0.47 degC, ±0.54 degC and ±0.017, respectively.

4. Result and Discussion

On the film-cooled surface, the heat transfer coefficient and the film-cooling effectiveness are defined as follows (Goldstein, 1971).

$$q=h(T_w-T_{aw}) \tag{1}$$

$$\eta=(T_{aw}-T_\infty)/(T_j-T_\infty) \tag{2}$$

The temperatures T_{aw}, T_∞ and T_j denote the adiabatic wall temperature, freestream temperature of the mainflow and injectant temparature, respectively. Most of the film-cooling studies have surveyed the heat transfer coefficient and the film-cooling effectiveness. In this study, however, the following dimensionless temperature was reported in the film-cooled boundary layer.

$$\theta=(T-T_\infty)/(T_j-T_\infty) \tag{3}$$

The temperature, T, stands for the temperature measured at each measuring point when the jets are injected. The bottom surface of the test injection plate was directly exposed to the hot injectant inside the plenum as in Fig. 1, so that heat can be transferred through the injection plate as in the actual film-cooled hot sections. In this steady-state conjugate heat transfer, the thermal conductivity ratio of the solid material to the ambient gas may be one of the most important parameters. For a typical modern turbine component, the thermal conductivity ratio of the turbine material at a nominal operating condition to the

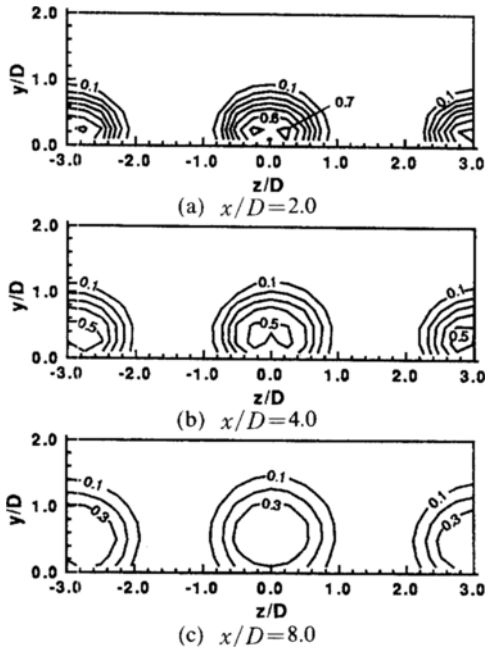

Fig. 2 Contours of dimensionless temperature, θ, for $M=1.0$ in the case of $\beta=0$ deg.

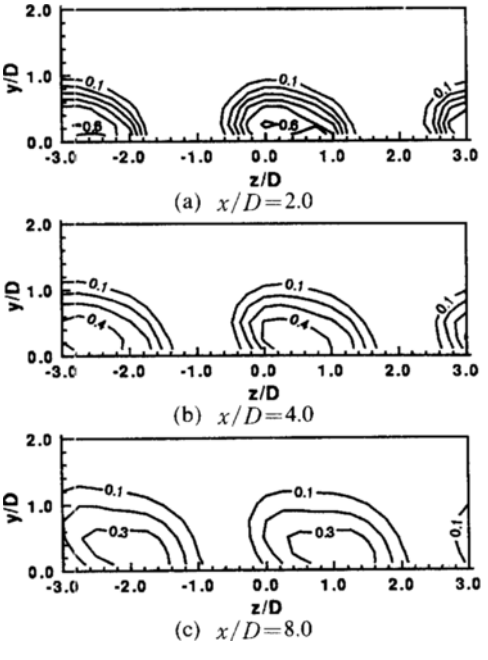

Fig. 3 Contours of dimensionless temperature, θ, for $M=1.0$ in the case of $\beta=30$ deg.

hot gas flow may be estimated about 300. The corresponding thermal conductivity ratio of the present experiment was about 50. Even though

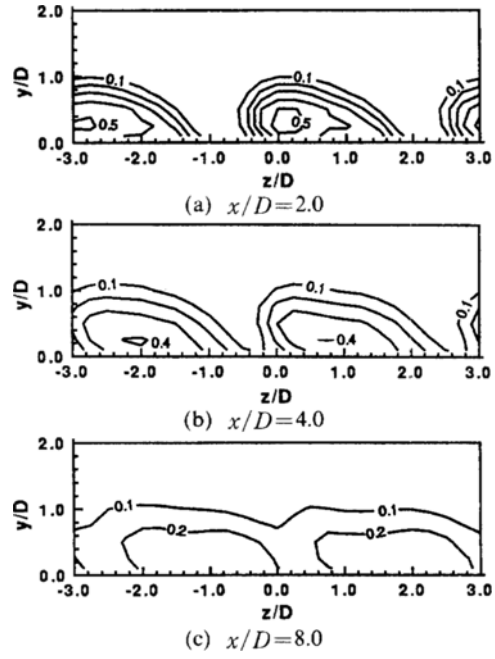

Fig. 4 Contours of dimensionless temperature, θ, for $M=1.0$ in the case of $\beta=60$ deg.

there was an apparent discrepancy between the two values, the backelite plate in this study seemed to be the best choice among available materials. If the present injection plate were assumed to be a good insulator, the dimensionless temperature measured on the wall, θ_w, could be identical to the adiabatic film-cooling effectiveness.

Downstream developments of the dimensionless temperature, θ, for $M=1.0$ are presented in Fig. 2~Fig. 5. The results show a good spanwise periodicity from jet to jet. When the jets are injected in the streamwise direction (Fig. 2), temperature distribution has a symmetry with respect to the x-y plane at $z/D=0.0$, and each region with higher dimensionless temperature is confined in the immediately downstream area of the injection hole. In the case of $\beta=30$ deg (Fig. 3), the temperature fields become asymmetrical and jet trajectories are shifted and somewhat extended in the positive z-direction, compared with those of the streamwise injection. As the orientation angle increases from 30 deg to 60 deg, the thermal field suffers relatively large change and each injectant is widely spread in the

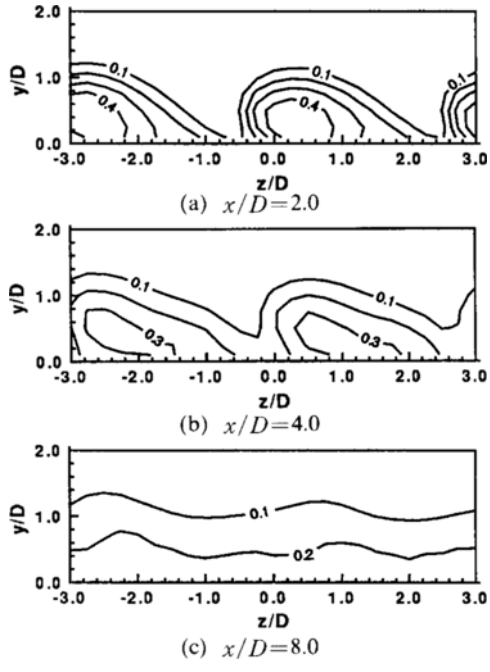

Fig. 5 Contours of dimensionless temperature, θ, for M=1.0 in the case of β=90 deg.

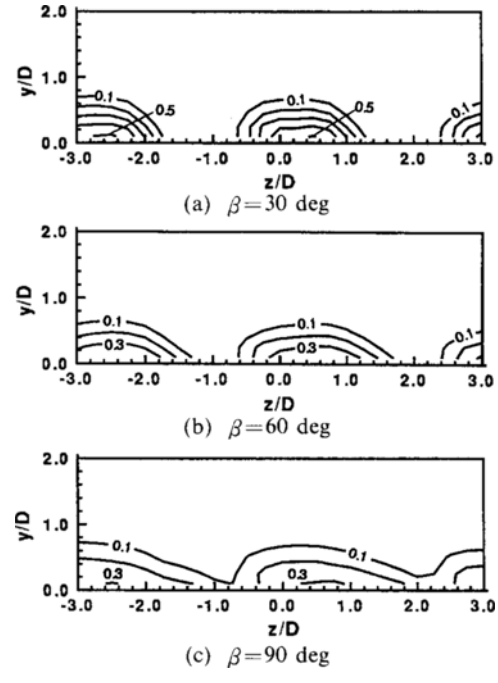

Fig. 6 Contours of dimensionless temperature, θ, at x/D=4 for M=0.5.

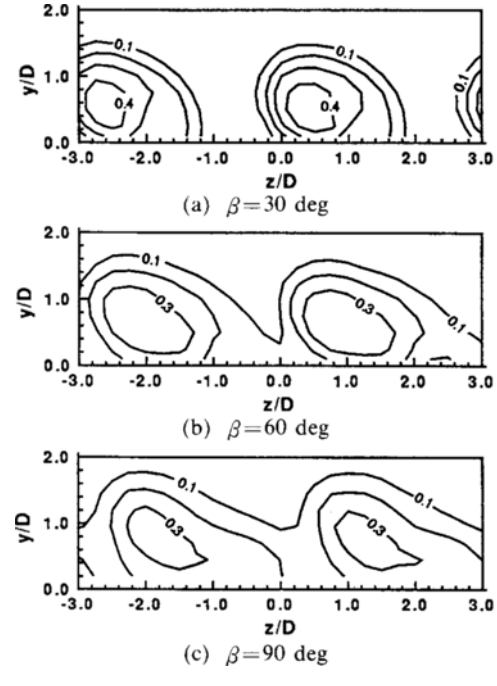

Fig. 7 Contours of dimensionless temperature, θ, at x/D=4 for M=1.5.

spanwise direction. When x/D is less than 4.0, neighboring injectants are not in contact and are not mixed with each other. When x/D reaches 8.0, however, the injectants from the neighboring holes come into contact and are vigorously mixed. In the case of β=90 deg (Fig. 5), the effect of the orientation angle is found to be strongest and the temperature contours are nearly parallel with the z-axis at x/D=8.0 as in Fig. 5(c). In general, the peak value of the dimensionless temperature and the temperature gradient rapidly decrease as the orientation angle increases. The wide spread of the injectants in the case of the large orientation angle results in an even temperature distribution in the spanwise direction. Ligrani et al. (1994b) also reported a wide spanwise spread of injectant and larger injectant concentration closer to the wall for the film cooling through a-row-of compound angle holes with $6D$ spacing. In this study, unifom film coverage occurs at smaller x/D, compared with their results.

Contours of the dimensionless temperature, θ, at x/D=4.0 for M=0.5 and M=1.5 are presented in Fig. 6 and Fig. 7, respectively. In order to understand the effect of the blowing ratio on the

downstream thermal field, the results in Fig. 3 (b), Fig. 4(b) and Fig. 5(b) are compared with those in Fig. 6 and Fig. 7. The blowing ratio has a significant effect on the temperature field. In the case of streamwise injection, increasing the blowing ratio promotes jet's separation from the film-cooled surface(Lee et al., 1994), which usually results in low film-cooling effectiveness. This tendency is also true for these compound angle injections as can be seen in Fig. 7. However, the increase in the blowing ratio expedites the interference between the neighboring jets as well as the mixing of the injectants with the mainflow. Therefore, larger blowing ratio results in more unifom temperature distribution. As the orientation angle increases for $M=0.5$ (Fig. 6), there seems to be no change in the jet area in the y-direction except for some spanwise dispersions of the injectants. When M increases to 1.5 (Fig. 7), jet's bounds are widely extended in the y-direction as well as in the z-direction and the locations of peak dimensionless temperature are apparently away from the wall, compared with those in Fig. 6. For this high blowing ratio, the increase in the orientation angle from 30 deg to 90 deg brings not only a large z-directional spread of the injectants but also a slight lift-off of each jet trajectory in the y-direction.

In the film-cooling, wall temperature on a film-cooled surface is one of the most important values, since it determines the life of a hot component. In this sense, the dimensionless near-wall temperature, θ_{nw}, based on the temperature measured at the closest position to the wall, i. e. at $z/D=0.1$, are introduced. These data can provide useful information since θ_{nw} can be a rough measure of the dimensionless wall temperature, θ_w, which is based on the wall temperature. It should be noted that θ_{nw} may be lower than θ_w for low blowing ratios, but higher than θ_w for higher blowing ratios. This is because the locations of maximum θ are usually found very near the wall below $y/D=0.1$ for the low blowing ratios as in the case of $M=0.5$ (Fig. 6), meanwhile for the blowing ratios higher than unity, the locations of maximum are observed above $y/D=0.1$ as can be seen in Fig. 7.

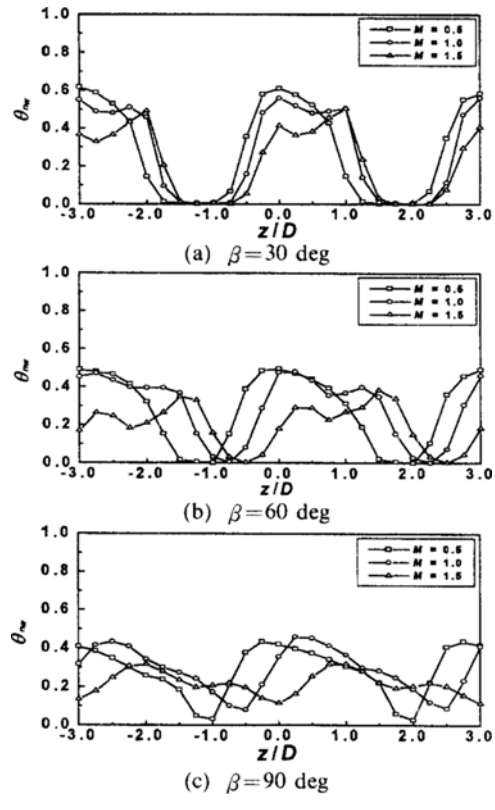

Fig. 8 Dimensionless near-wall temperature at $y/D=0.1$, θ_{nw}, at $x/D=2.0$.

The spanwise θ_{nw}-variations at $x/D=2.0$ are presented in Fig. 8 as a function of the blowing ratio. At this near-hole location, there exist relatively large variations of θ_{nw} in the z-direction, and the spanwise variation diminishes as the blowing ratio and orientation angle increase. The most uniform distributions of θ_{nw} are always found in the case of $\beta=90$ deg, for all blowing ratios. When the orientation angle is less than 60 deg, each jet region can be clearly identified. In the case of $\beta=90$ deg for $M=1.5$, however, it is very hard to distinguish a jet region from the mainflow region even at this near-hole location. The θ_{nw}-profiles measured at $x/D=8.0$ (Fig. 9) show that in general the compound angle injection provides remarkably even temperature distributions compared with those in Fig. 8. However, even at this location, there still exist large variations of θ_{nw} in the case of $\beta=30$ deg. It is interesting that in the cases of $\beta=60$ deg and $\beta=90$ deg,

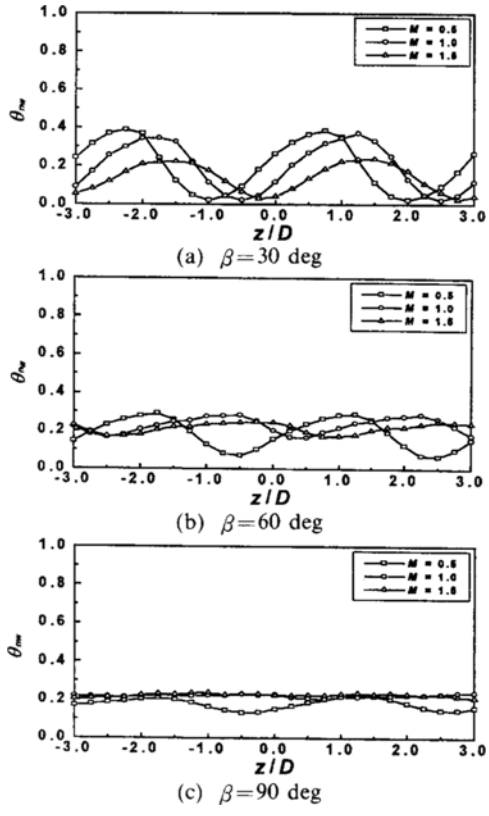

Fig. 9 Dimensionless near-wall temperature at $y/D=0.1$, θ_{nw}, at $x/D=8.0$.

θ_{nw}'s for $M=1.0$ have nearly the same values as those for $M=1.5$, even though the added masses are different. The θ_{nw}-profiles at $x/D=8.0$ as a function of the orientation angle (Fig. 10) reveal that for $M=0.5$, the θ_{nw}-profile is strongly dependent upon the orientation angle but in the case that the orientation angle is larger than 60 deg, the variations of θ_{nw} are relatively small. When the orientation angle is larger than 60 deg, θ_{nw} for $M=1.5$ is nearly independent of the orientation angle, although there is still large change in the θ_{nw}-profile when the orientation angle is smaller than 30 deg. For this high blowing ratio, the spanwise-averaged value of θ_{nw} in the case of $\beta=$ 60 deg seems to be nearly the same as that in the case of $\beta=90$ deg, which is approximately equivalent to the peak values of θ_{nw} when the orientation angles are 0 deg and 30 deg. The most uniform θ_{nw}-profile is encountered in the case of $\beta=90$ deg for $M=1.5$.

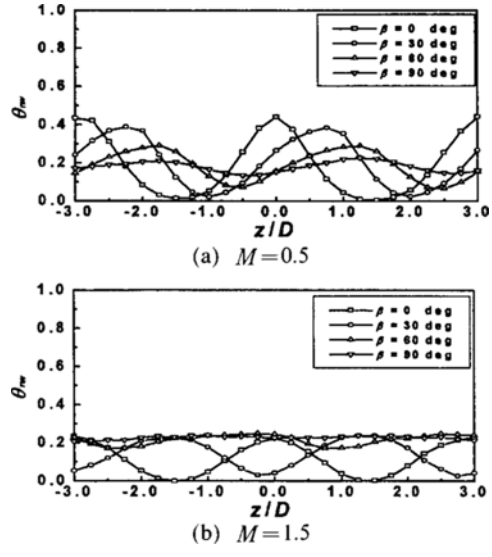

Fig. 10 Dimensionless near-wall temperature at $y/D=0.1$, θ_{nw}, at $x/D=8.0$ as a function of β.

5. Conclusion

Detailed measurements of temperature within the heated film-cooling jets with compound angle orientations have been conducted for four orientation angles of 0 deg, 30 deg, 60deg and 90 deg with three blowing ratios of 0.5, 1.0 and 1.5. The inclination angle, span-to-diameter ratio and length-to-diameter of the injection holes are fixed at 30 deg, 3.0 and 4.0, respectively, throughout the whole experiments. The results in this study are summarized as follows.

In general, with an increment of the orientation angle, the downstream thermal field becomes asymmetrical, and each injectant is shifted and spread in the spanwise direction. This tendency rapidly grows as the blowing ratio increases. When the blowing ratio is low, the orientation angle has an small effect on the temperature field and the spanwise spread of each injectant is found to be relatively small. Therefore, each jet region is confined to a restricted area near the wall surrounded by the mainflow. When the blowing ratio is higher than unity, however, each jet region is widely extended in the spanwise direction with a slight lift-up of the jet trajectory, as the orientation angle increases. When the orienta-

tion angle is large for the blowing ratios higher than unity, each jet bound easily touches the neighboring ones and each injectant is vigorously mixed with the neighboring ones as well as the mainflow. In this case, the most uniform coverage of the injectants is attained.

Near-wall temperature profiles show that larger orientation angle provides better film-cooling performance and also improves uniform film coverage. The effect of the compound angle injection is found to be dominant in the case that the orientation angle is larger than 60 deg, especially when the blowing ratio is higher than unity. When the orientation angle is less than 30 deg, however, there still exist considerable spanwise variations in the near-wall temperature for all blowing ratios.

Acknowledgement

The research herein was supported by the Korea Science and Engineering Foundation (KOSEF Grant Number 95-0200-12-01-3), and was also partly supported by Turbo and Power Machinery Research Center.

References

Goldstein, R. J., 1971, "Film Cooling," Advances in Heat Transfer, edited by T. Irvine and J. P. Hartnett, Academic Press, New York, Vol. 7, pp. 272~328.

Honami, S., Shizawa, T. and Uchiyama, A., 1994, "Behavior of the Laterally Injected Jet in Film Cooling: Measurements of Surface Temperature and Velocity/ Temperature Field Within the Jet," *ASME Journal of Turbomachinery*, Vol. 116, pp. 106~112.

ISO 5167-1:1991(E), 1991, Measurement of Fluid Flow by Means of Pressure Differential Devices- Part1: Orifice Plates, Nozzles and Venturi Tubes Inserted in Circular Cross-Section Conduits Running Full, International Organization for Standardization.

Kline, S. J. and McClintock, F. A., 1953, "Describing Uncertainties in Single Sample Experiments," *Mechanical Engineering*, Jan., pp. 3~8.

Lee, S. W., Lee, J. S. and Ro, S. T., 1994, "Experimental Study on the Flow Characteristics of Streamwise Inclined Jets in Crossflow on Flat Plate," *ASME Journal of Turbomachinery*, Vol. 116, pp. 97~105.

Lee, S. W., Kim, Y. B. and Lee, J. S., 1997, "Flow Characteristics and Aerodynamic Losses of Film-Cooling Jets With Compound Angle Orientations," ASME *Journal of Turbomachinery*, Vol. 119, pp. 310~319.

Ligrani, P. M., Ciriello, S., and Bishop, D. T., 1992, "Heat Transfer, Adiabatic Effectiveness, and Injectant Distributions Downstream of a Single Row and Two Staggered Rows of Compound Angle Film-Cooled Holes," ASME *Journal of Turbomachinery*, Vol. 114, pp. 687~700.

Ligrani, P. M., Wigle, J. M., Ciriello, S. and Jackson, S. W., 1994a, "Film-Cooling from Holes with Compound Angle Orientations: Part 1 - Results Downstream of Two Staggered Rows of Holes with 3D Spanwise Spacing," ASME *Journal of Heat Transfer*, Vol. 116, pp. 341~352.

Ligrani, P. M., Wigle, J. M. and Jackson, S. W., 1994b, "Film-Cooling from Holes with Compound Angle Orientations: Part 2 - Results Downstream of a Single Row of Holes with 6*D* Spanwise Spacing," ASME *Journal of Heat Transfer*, Vol. 116, pp. 353~362.

Srinath, V. E., Dyrk, Z. and Han, J. C., 1995a, "Heat Transfer Coefficients over a Flat Surface With Air and CO_2 Injection Through Compound Angle Holes Using a Transient Liquid Crystal Image Method," to appear in ASME *Journal of Turbomachinery*, ASME paper 95-GT-10.

Srinath, V. E., Dyrk, Z. and Han, J. C., 1995b, "Film Effectiveness over a Flat Surface with Air and CO_2 Injection Through Compound Angle Holes Using a Transient Liquid Crystal Image Method," to appear in ASME *Journal of Turbomachinery*, ASME paper 95-GT-11.

STP 470A, 1974, Manual on the Use of Thermocouples in Temperature Measurement, published by ASTM.